Title: CXCL16 mediates nociception and inflammation in murine post-traumatic osteoarthritis

Authors: Lindsey Lammlin[1,2], Stephen Redding[2], Alexander J. Knights[2,3], Aanya Mohan[1,2], Michael D. Newton[2], Rachel F. Bergman[2], Isabelle J. Smith[2], Scarlet C. Howser[2], Sofia Gonzalez-Nolde[2], Phillip M. Rzeczycki[2], Natalie S. Adamczyk[4], Rachel E. Miller[4], *Tristan Maerz[1,2,5,6]

Affiliations:

[1]ETH Zürich, Zürich, Switzerland

[2]Department of Orthopaedic Surgery, University of Michigan; Ann Arbor, Michigan, United States.

[3]Washington University St. Louis, St. Louis, Michigan

[4]Division of Rheumatology, Rush University Medical Center; Chicago, Illinois, United States.

[5]Department of Biomedical Engineering, University of Michigan; Ann Arbor, Michigan, United States.

[6]Division of Rheumatology, Department of Internal Medicine, University of Michigan; Ann Arbor, Michigan, United States.

Corresponding Author Info

*Tristan Maerz, PhD
ETH Zürich, Zürich, Switzerland.

tristan.maerz@hest.ethz.ch

Gloriastrasse 39, 8092 Zürich, Switzerland

One Sentence Summary:

CXCL16 regulates synovial inflammation and mediates joint nociception via CXCR6, highlighting its potential as a therapeutic target for post-traumatic osteoarthritis.

Abstract:

This study investigates the role of the chemokine CXCL16 and its receptor, CXCR6, in post-traumatic osteoarthritis (PTOA) and joint nociception, highlighting the potential of targeting the CXCL16-CXCR6 axis for therapeutically managing joint inflammation and pain. Following joint injury in mice, the CXCL16-CXCR6 signaling axis is activated in synovium, driven by synovial fibroblasts and macrophages. Human OA synovium also exhibited increased CXCL16 and CXCR6 gene expression. CXCL16 stimulated a pro-inflammatory response in fibroblasts and macrophages, contrasting with an anti-inflammatory response observed in mesenchymal progenitor cells. In mice, repeated intra-articular CXCL16 injections induced histological synovitis and sex-dependent activation of inflammatory and fibrotic transcriptional programs in synovium. Repeated CXCL16 joint injections also induced knee hyperalgesia, which was mitigated by co-administration of the CXCR6 antagonist, ML339. A single intra-articular injection of CXCL16 induced acute knee hyperalgesia as early as 30 minutes post-injection, which was completely abrogated by ML339 co-treatment, suggesting direct CXCL16 binding to nociceptor-expressed CXCR6. In a murine PTOA model, systemic CXCR6 antagonism with ML339 alleviated knee hyperalgesia and altered circulating immune cell profiles. Direct stimulation of mouse dorsal root ganglion-derived nociceptive neurons with CXCL16 induced rapid calcium signaling, which was abolished by co-treatment with ML339. These findings establish CXCL16 as a regulator of joint inflammation and identifies the CXCL16-CXCR6 binding mechanism as key in mediating pain-related behaviors and nociceptor activation, offering a therapeutic target for PTOA-related inflammation and pain management.

Main text:

INTRODUCTION

The role of synovitis in promoting multiple pathological manifestations of osteoarthritis (OA), including pain and catabolic articular destruction, is now well-recognized(*1*, *2*). In idiopathic OA, synovitis manifests as chronic low-grade tissue inflammation with intermittent flare-ups, and recent literature has demonstrated the existence of different inflammatory endotypes in both late-stage OA and rheumatoid arthritis (RA)(*3–5*). In the setting of post-traumatic osteoarthritis (PTOA), joint injury results in a high degree of acute synovial inflammation, which transitions to a chronic, low-grade nature akin to that observed in idiopathic OA.

A highly coordinated and tightly regulated set of factors orchestrate the local and systemic responses to tissue trauma. However, the immunological mechanisms underpinning joint injury-induced synovitis and its downstream consequences remain poorly described. Among the factors strongly induced following injury are the families of chemokines, secreted by tissue-resident stromal, endothelial, and immune cells. While some chemokines such as CCL2/MCP-1(*6–10*) have been shown to be involved in OA/PTOA inflammation, the individual functions of most chemokines remain unclear in the context of joint injury and PTOA development. For instance, while CCL5/RANTES was shown to activate IL6 production in human synovial fibroblasts(*11*), indicating a potential deleterious pro-inflammatory effect, its genetic ablation did not alter disease severity in a surgical mouse OA model(*12*). Here, we identified and functionally characterized the chemokine CXCL16 as a synovial-derived factor selectively upregulated and secreted following joint injury. CXCL16 is expressed as a transmembrane protein, and it is cleaved from the cell surface by a disintegrin and metalloproteinase 10 (ADAM10) to act as a soluble ligand(*13*). As a transmembrane protein, CXCL16 is thought to act as an adhesion molecule for leukocytes(*14*) and can also act as a receptor for the soluble ligand form of CXCL16(*15*, *16*). CXCL16 also binds CXCR6, a G-protein coupled receptor and the only classical receptor described to interact with CXCL16(*17*, *18*). The CXCL16-CXCR6 axis has been associated with *in vivo* chemotaxis of macrophages, MSCs, and T cells in lung, liver, cardiac, renal, skin, and rheumatoid arthritic joint tissues(*19–24*). In the context of RA, CXCL16 has been shown to recruit mononuclear cells to synovial

79 tissue(*25*) and promote FLS proliferation(*26*). CXCL16 has also been shown to be involved in
80 the recruitment of endothelial progenitor cells, contributing to pathological angiogenesis
81 observed in RA(*27*). Ablation of CXCR6 ameliorated K/BxN serum-induced arthritis by
82 mitigating inflammatory cell infiltration, and fewer T cells and macrophages were found in joints
83 of K/BxN-challenged CXCR6$^{-/-}$ mice(*27*). CXCL16 monoclonal antibody treatment was also
84 shown to be effective in mitigating collagen induced arthritis in mice(*28*). Despite this evidence
85 from inflammatory and autoimmune-mediated arthritis, no prior study has described the role of
86 the CXCL16-CXCR6 axis following joint injury and during PTOA progression.

87 Chemokines are also highly relevant in the context of pain, and pain mechanisms in
88 OA/PTOA remain poorly described. Chemokines can either directly affect nociception as
89 agonists of nerve fiber-bound receptors, serving to sensitize nociceptive transmission
90 underpinning pain, or indirectly by inducing the upregulation of cytokines and neurotrophic
91 mediators that interact with neurons(*29*, *30*). Very few chemokines have been characterized in
92 their involvement in joint nociception and OA/PTOA-related pain specifically. In a mouse model
93 of gouty arthritis, the CXCL5-CXCR2 axis was shown to have a role in pain and neurogenic
94 inflammation as mice with neuronal specific CXCR2 depletion exhibited less severe pain
95 related-behaviors and reduced production of calcitonin gene-related peptide and substance P(*31*).
96 Prior work has demonstrated that CCL2 is a key mediator of joint nociception by interacting with
97 nociceptor-bound CCR2(*6*). Furthermore, CCL2$^{-/-}$ and CCR2$^{-/-}$ mice exhibit delayed onset of
98 pain-related behavior in a surgical PTOA model(*7*, *8*). The CXCL16-CXCR6 axis, however, has
99 yet to be described in the context of joint nociception.

100 The objective of this study was to assess the role of CXCL16 in joint injury-induced,
101 PTOA-associated inflammation and nociception. We demonstrate that the CXCL16-CXCR6 axis
102 is activated following traumatic joint injury, that CXCL16 induces pro-inflammatory signaling in
103 synovial fibroblasts and macrophages, and that CXCL16 is sufficient by itself to induce joint
104 pain and synovitis in mice *in vivo*. Using *in vitro* Ca^{2+} measurements in neuronal cells derived
105 from nociceptor-specific GCaMP6s calcium sensor mice and using *in vivo* acute hyperalgesia
106 experiments, we show that CXCL16 directly agonizes nociceptors and induces knee
107 hyperalgesia. Finally, employing a clinically-relevant pharmacological CXCR6 antagonist, we
108 demonstrate that CXCR6 inhibition mitigated the pro-algesic effects of CXCL16, abrogated

109 CXCL16-induced Ca^{2+} signaling by nociceptors, and ameliorated joint injury-induced knee
110 hyperalgesia.

111 **RESULTS**

112 *Traumatic joint injury activates the CXCL16-CXCR6 axis in synovium*

113 To understand the temporal expression patterns of synovial-derived chemokines and their
114 receptors following joint injury, we analyzed our bulk RNA-sequencing (RNA-seq) data of
115 whole mouse synovium (inclusive of Hoffa's fat pad)(*32*). We observed marked injury-induced
116 perturbation in members of the CCL and CXCL families (**Fig. 1A**), with corresponding changes
117 in the expression pattern of their respective receptors (**Fig. S1**). We next screened this list for
118 chemokines with zero or near-zero expression in Sham joints, further focusing on chemokines
119 with no prior PTOA-related studies. We identified CXCL16, which was upregulated 4.22- and
120 2.97-fold at 7d and 28d post-ACLR, respectively, with markedly lower P_{adj} values compared to
121 all other chemokines (**Fig. 1A**). qPCR corroborated the upregulation of *Cxcl16* at additional
122 timepoints post-ACLR in the synovium and meniscus (**Fig. S2A-B**). CXCL16 is expressed as a
123 transmembrane protein, in which state it can function as a scavenger receptor for lipoproteins
124 and bacteria(*33*) in addition to acting as a receptor for the soluble form of CXCL16(*15*, *16*).
125 Upon cleavage by ADAM10, CXCL16 is shed from the membrane and acts as a soluble
126 chemokine, shown to mediate leukocyte chemotaxis(*14*) as well as activate the
127 phosphatidylinositol-4,5-bisphosphate 3-kinase (PI3K)-Akt/PKB and extracellular signal-
128 regulated kinase mitogen-activated protein kinase (ERK/MAPK) pathways, and mobilize Ca^{2+}
129 via the G protein-coupled receptor CXCR6(*34*). Mining of our previously published bulk RNA-
130 seq data of whole synovium also showed that *Cxcr6* was upregulated 3.30-fold at 7d and 2.87-
131 fold at 28d post-ACLR (**Fig. S1A**). By qPCR we also observed upregulation of *Adam10* in the
132 synovium, but not the meniscus following joint injury (**Fig. S2A-B**), demonstrating upregulation
133 of the entire CXCL16-CXCR6-ADAM10 axis following joint injury.

134 In a meta-analysis of transcriptomic data of human OA synovium, we also observed
135 marked alterations in the expression patterns of CCL and CXCL chemokines and their receptors,
136 relative to healthy synovium (**Fig. S1B-C**). *CXCL16*, *CXCR6*, and *ADAM10* were significantly
137 upregulated in OA synovium compared to healthy synovium (**Fig. 1B**). Notably, CXCL16 had
138 the lowest, i.e. most significant composite P_{adj} value compared to all other CCL and CXCL

139 chemokines (**Fig. S1B**), demonstrating that CXCL16 upregulation is also observed in human OA
140 and not confined to the acute post-injury period. Uninjured mouse joints and healthy human OA
141 synovium exhibited very low CXCL16 expression. Concordantly, while CXCL16 protein was
142 undetectable in the synovial fluid of uninjured joints, the synovial fluid of injured ACLR joints
143 was enriched in CXCL16 protein (**Fig. 1C**).

144 To identify the synovial cells expressing CXCL16 (intracellular) and CXCR6 (surface)
145 proteins, we performed flow cytometry of ACLR synovium compared to healthy contralateral
146 synovium at both early (3d) and intermediate (14d) timepoints following injury. We observed
147 large but statistically non-significant increases in the total number of CXCL16+ and CXCR6+
148 cells in ACLR synovia compared to uninjured synovia (**Fig. 1D**), but only CXCR6+ cells
149 increased in their proportion to all live cells at 3d post-ACLR (**Fig. 1E**). This is likely due to the
150 widely reported dramatic increase in total synovial cells after joint injury, corroborated by our
151 results showing all major synovial cell types elevated at 3d and 14d post-ACLR compared to
152 contralateral tissue (**Fig. S2C-G**). Intracellular CXCL16 was found to be expressed most
153 strongly by CD31(-) CD45(-) stromal cells, i.e. synovial fibroblasts, as well as by CD31(+)
154 CD45(-) endothelial cells, and by CD45(+) immune cells (**Fig. 1F**). Within CD45(+) immune
155 cells, we observed CXCL16 expression in CD11b(+) CD64(+) macrophages, CD11b(-) CD3(+)
156 T cells, and other immune subsets (**Fig. 1G**). CXCR6 was predominantly expressed by immune
157 cells with lower levels of expression in stromal and endothelial cells (**Fig. 1F**). The CXCR6+
158 immune cells were comprised of ~80-90% macrophages (**Fig. 1G**). Mining of our previously
159 published murine synovial single-cell RNA sequencing data(*35*) shows that *Cxcl16* transcript is
160 expressed by fibroblasts and most highly in macrophage and dendritic cells, whereas *Cxcr6*
161 transcripts are confined to T-cells, and *Adam10* is expressed ubiquitously across synovial cell
162 populations (**Fig. 1H**).

163 Taken together, these findings demonstrate that CXCL16 is a disease-specific secreted
164 factor, expressed by synovial fibroblasts and macrophages, and enriched in the synovium of both
165 human OA patients and injured mouse joints.

166 *IL1β and TNFα induce CXCL16 expression in joint relevant cell types*

167 Given the observation of injury-induced upregulation of CXCL16 by multiple synovial
168 cell types, we sought to identify upstream activators of CXCL16 expression (**Fig. 2A**). We found

169 that IL-1β and TNFα, two key cytokines strongly upregulated in synovium following ACLR(*32*,
170 *36*), activated *Cxcl16* and *Cxcr6* transcript upregulation in both primary murine FLS and bone
171 marrow-derived macrophages (**Fig. 2B-C**). IL-1β and TNFα also caused upregulation of *Adam10*
172 in FLS (**Fig. 2B**), but downregulation of *Adam10* in BMDM (**Fig. 2C**). We confirmed the
173 increase of secreted CXCL16 protein in the conditioned medium of IL-1β- and TNFα-treated
174 FLS, compared to vehicle-treated cells (**Fig. 2B**). We also found IL-1β and TNFα to cause
175 upregulation of *Cxcr6* in an immortalized chondrogenic cell line, ATDC5s - a culture model of
176 articular chondrocytes, whereas these cytokines induced downregulation of *Adam10* while
177 *Cxcl16* remained unchanged (**Fig. 2D**). These results demonstrate that the CXCL16-CXCR6 axis
178 is activated by IL1β and TNFα.

179 *CXCL16 induces cell type-dependent pro- or anti-inflammatory gene expression*

180 We next wanted to assess the potential functional role of CXCL16 in joint-relevant cell
181 types. We treated primary murine synovial fibroblasts, bone marrow-derived macrophages, and
182 bone marrow-derived mesenchymal progenitor cells (BMPCs) with increasing doses of
183 recombinant CXCL16 protein. We found CXCL16 to induce a multi-factorial pro-inflammatory
184 response in FLS, indicated by both an increase in pro-inflammatory gene expression (*Il1b, Il6*)
185 and a decrease in anti-inflammatory gene expression (*Il10*) (**Fig. 3A**). BMDMs treated with
186 CXCL16 similarly had a similar double-edge pro-inflammatory response as summarized by the
187 increase in macrophage polarization score upon treatment with CXCL16 (**Fig. 3B**). This
188 macrophage score is an aggregate assessment of macrophage phenotype which is calculated by
189 the ratio of pro-inflammatory (*Il1b*, *Il6*, *Mmp1b*) to anti-inflammatory (*Cd206*, *Il4*, *Il10*) gene
190 expression (**Fig. S3A-B**). Interestingly, CXCL16 elicited a cell-type specific response as BMPCs
191 treated with CXCL16 upregulated their expression of anti-inflammatory transcripts *Il10* and
192 *Il1ra*, and the pro-inflammatory transcript *Il1b*, but *Il6* was unchanged (**Fig. 3C**).

193 In addition to promoting cell-type specific inflammatory responses, CXCL16 contributed
194 to its own feed forward signaling activation in FLS, BMDM, and BMPCs. CXCL16-treated FLS
195 upregulated *Cxcl16*, *Cxcr6*, and *Adam10* expression (**Fig. 3A**). BMDMs exhibited similar
196 responses, with increases in *Cxcl16*, *Cxcr6*, and *Adam10* expression after treatment with
197 recombinant CXCL16 (**Fig. 3B**). BMPCs exhibited strong upregulation of *Cxcr6* with a less
198 dramatic induction of *Cxcl16* and *Adam10* (**Fig. 3C**). In an *in vitro* migration assay, BMDMs and

199 BMPCs also exhibited a dose-dependent chemotactic response to CXCL16 (**Fig. 3D**),
200 corroborating prior studies on the chemotactic effects of CXCL16(*19–24*). Taken together, these
201 *in vitro* findings demonstrate that CXCL16 induces pro-inflammatory effects in primary FLS and
202 BMDMs but anti-inflammatory effects in BMPCs.

203 *Repeated intra-articular injections of CXCL16 induces knee hyperalgesia via CXCR6 and*
204 *synovitis in healthy murine joints*

205 On the basis of CXCL16 activating pro-inflammatory gene expression in synovial
206 fibroblasts and BMDMs, we next wanted to assess whether CXCL16 is sufficient by itself to
207 induce synovitis and joint disease *in vivo*. We injected either 5 µL of vehicle or 0.25 ng (low
208 dose) or 25 ng (high dose) of recombinant murine CXCL16 into healthy, adult C57BL/6 knee
209 joints for five consecutive days and performed knee hyperalgesia and histological assessments.
210 Low and high dose CXCL16-injected limbs, but not vehicle-injected limbs, exhibited reduced
211 knee withdrawal thresholds at 7d following the first injection, indicative of hyperalgesia (**Fig.**
212 **4A**). High dose CXCL16-injected limbs had a sustained reduction in knee withdrawal threshold
213 up to 14d following the first injection, but this effect was not observed in low dose or vehicle-
214 injected limbs (**Fig. 4A**). Histological evaluation demonstrated no change in the total post-
215 traumatic osteoarthritis score, however there were significantly increased total synovitis scores in
216 CXCL16-injected joints, driven by increased synovial lining hyperplasia and synovial fibrosis
217 (**Fig. 4B-C**).

218 To assess the molecular programs that underpin these pathological manifestations, we
219 performed bulk RNA-seq of whole synovium from a separate cohort of mice treated with the
220 identical vehicle or high-dose CXCL16 injection regimen as above. In this cohort, CXCL16-
221 injected joints again exhibited reduced knee withdrawal thresholds 7d post-first injection (**Fig.**
222 **4D**). By RNA-seq at the same timepoint, we observed a highly sex-dependent perturbation of the
223 synovial transcriptome due to CXCL16 administration (**Fig 4E**). Whereas female synovium
224 exhibited near-absent CXCL16-induced differentially expressed genes (DEGs), male synovia
225 upregulated cytokines, chemokines, and cytokine/chemokine receptors (e.g. *Ccl2, Ccl7, Cxcl5,*
226 *Il1rl1, Ccr5*), genes of macrophage-relevant transcription factors and genes related to
227 macrophage polarization (e.g. *Junb, Fos, Mt1, Arg1, Fgr*), and genes related to fibroblast
228 activation and ECM turnover (*Pdpn, Mmp3, Itga5, Lum, Cspg4, Hmcn2*) (**Fig. 4E, Data file S2**).

229 GSEA pathway analysis demonstrated that synovia from male CXCL16-treated joints had
230 enriched pathways related to collagen production, immune/inflammatory response, and
231 neuroinflammation (**Fig. 4F**). Taken together, these findings demonstrate that CXCL16 is
232 sufficient by itself to induce arthritis-relevant disease manifestations in healthy joints *in vivo*,
233 characterized by increased hyperalgesia, histological synovitis, and the induction of a synovial
234 transcriptional program indicative of inflammation, lymphocyte and macrophage activation,
235 ECM production, and fibroblast proliferation.

236 To interrogate the receptor mechanism by which CXCL16 induced pain, we co-
237 administered a CXCR6-specific antagonist, ML339, in the same repeated injection study design.
238 Male mice were administered five consecutive days of intra-articular vehicle, CXCL16 (200 ng),
239 or CXCL16 (200 ng) + ML339 (1 mM) injections. CXCL16-injected joints again had reduced
240 knee withdrawal thresholds and knee withdrawal threshold ratios as compared to vehicle injected
241 limbs. This hyperalgesia-inducing effect was partially ablated by co-administration of ML339, as
242 joints injected with combinatorial CXCL16 + ML339 had significantly higher knee withdrawal
243 threshold and knee withdrawal ratio compared to joints injected with CXCL16 only (**Fig. 4G**).

244 *CXCL16 induces acute knee hyperalgesia via CXCR6*

245 Joint pain is a complex physiological process orchestrated by multiple cell types, ligands,
246 and receptors. A given mediator may agonize pain pathways via direct signaling, i.e. binding to
247 joint nociceptor-bound receptors to directly alter nociception, or via indirect means, i.e. inducing
248 the expression of other factors that directly bind nociceptors. Having demonstrated that CXCL16
249 is sufficient to induce knee hyperalgesia in a repeated-injection model, we sought to assess
250 whether this at least partially occurs via direct interactions with joint-innervating nociceptors.
251 We performed an acute hyperalgesia experiment in which recombinant CXCL16 (25 ng), or
252 vehicle (sterile PBS) was injected into joints followed by knee withdrawal threshold
253 measurements at acute timepoints post-injection (30 mins – 4 hrs) (**Fig. 5A**). Vehicle injection
254 caused minor decreases in knee withdrawal threshold compared to baseline, however, CXCL16
255 significantly reduced withdrawal thresholds compared to vehicle by 30 mins post-injection in
256 male mice, with a sustained effect until 7 days (**Fig. 5B-C, Fig. S4A-B**). Strikingly, despite
257 female mice also exhibiting increased hyperalgesia after repeated injections in the prior
258 experiment (**Fig. 4A, D**), female mice had absent hyperalgesia responses relative to vehicle in

259 the acute experiment (**Fig. 5B-C**, **Fig. S4A-B**). The rapid responses observed in this experiment
260 provide evidence of a direct nociceptive effect, i.e. direct interactions between CXCL16 and
261 nociceptor-bound receptors(*37*, *38*).

262 We next wanted to ascertain whether the induction of acute hyperalgesia by CXCL16 is
263 mediated by CXCR6. We conducted another acute hyperalgesia experiment in only male mice
264 with a higher dose of CXCL16 (250 ng) and intra-articular co-administration of either vehicle or
265 the CXCR6 antagonist ML339 (1mM) (**Fig. 5D**). Consistent with the prior experiment, CXCL16
266 induced acute hyperalgesia that persisted until 24 hrs post-injection, and co-administration of
267 ML339 completely ablated this response (**Fig. 5E-F, Fig. S4C-D**). These findings demonstrate
268 that CXCL16-induced hyperalgesia is mediated via CXCR6 binding.

269 *Systemic CXCR6 antagonism blocks joint injury-induced hyperalgesia*

270 As joint injury induces the upregulation of multiple cytokines, chemokines, and
271 neurotrophic mediators (**Fig. 1A**)(*32*) that orchestrate synovitis and hyperalgesia, we next
272 wanted to assess whether CXCR6 antagonism mitigates injury-induced hyperalgesia. Male mice
273 underwent ACLR and received 5x intra-peritoneal injections of ML339 (5 mg/kg) or vehicle
274 followed by assessments of knee hyperalgesia and circulating immune cell populations (**Fig.**
275 **5G**). At the study endpoint, 7d post-ACLR, we also conducted an acute hyperalgesia experiment
276 to measure any potential acute analgesic effects due to systemic injection. Whereas pre-injection
277 withdrawal thresholds were comparable between treatment groups, ML339-treated mice had
278 significantly higher withdrawal threshold ratio and absolute withdrawal threshold 2 hrs post-
279 injection. (**Fig. 5H-I, Fig. S4E-F**). Complete blood counts further revealed that ML339-treated
280 mice had higher circulating total white blood cell and neutrophil counts (**Fig. 5J**). These findings
281 indicate that systemically administered ML339 acutely mitigates ACLR-induced knee
282 hyperalgesia.

283 *CXCL16 induces rapid Ca^{2+} influx in dorsal root ganglia-derived nociceptive neurons via*
284 *CXCR6*

285 Given our observation that CXCR6 antagonism mitigated CXCL16-induced acute
286 hyperalgesia as well as joint injury-induced hyperalgesia, we last sought to determine whether
287 CXCL16 directly agonizes nociceptive neurons and whether this requires CXCR6. We isolated

288 and cultured primary neurons derived from the dorsal root ganglia (DRG) of $Na_V1.8$-Cre;
289 $GCaMP6s^{fl/+}$ mice, which express the fluorescent calcium indicator, GCaMP6s, in nociceptive
290 neurons, marked by expression of the voltage-gated sodium channel 1.8 ($Na_V1.8$)(*39*). In a time
291 series experiment, cultured neurons were first treated with a negative control (vehicle only),
292 followed by a single dose of 50 ng/ml CXCL16, with KCl used as a positive control (**Fig. 6A**).
293 This was conducted in the presence or absence of 180 μM ML339 to antagonize CXCR6, and
294 fluorescent signal was monitored and quantified as the change over baseline. CXCL16, but not
295 vehicle, induced fluorescent responses, indicative of rapid neuronal Ca^{2+} signaling (**Fig. 6B-D**).
296 Co-treatment with the CXCR6 antagonist ML339 completely ablated CXCL16-induced
297 fluorescent responses ($P<0.0001$), with no effect on positive control responses to KCl (**Fig. 6B-**
298 **D**). Taken together, these findings confirm that CXCL16 directly agonizes nociceptive neurons
299 by inducing Ca^{2+} signaling, and this effect is abolished by pharmacological inhibition of the
300 CXCR6 receptor.

301 **DISCUSSION:**

302 This study elucidated the role of the CXCL16-CXCR6 axis in the context of post-
303 traumatic osteoarthritis (PTOA), with a focus on its contributions to inflammation and
304 nociception. Our findings demonstrate that joint injury rapidly activates gene and protein
305 expression of CXCL16 and CXCR6, and that CXCL16 orchestrates synovial inflammation, pain-
306 related behaviors and nociceptive signaling during PTOA progression. Using a translationally-
307 relevant small-molecule antagonist against CXCR6, we confirmed that CXCR6 mediates
308 CXCL16-induced joint hyperalgesia *in vivo* as well as CXCL16-induced Ca^{2+} signaling in DRG-
309 derived nociceptive neurons *in vitro*.

310 To our knowledge, this is the first study to demonstrate the role of CXCL16 and its only
311 known classical receptor, CXCR6, in peripheral nociception. Recently, Wang, et. al.,
312 demonstrated that CXCL16 expression and CXCL16 mRNA N^6-methyladenosine modification
313 was increased in rat sympathetic ganglia in a model of spared nerve injury (SNI)-induced
314 neuropathic pain(*40*). They further showed that intra-DRG administration of CXCL16 induced
315 mechanical allodynia in naïve rats while ablation of CXCL16 in sympathetic ganglia mitigated
316 SNI-induced mechanical allodynia, establishing a role for CXCL16 in mediating neuropathic
317 pain(*40*). Wang, et. al., also observed CXCR6 protein expression in rat DRG neurons(*40*), which

318 suggests that CXCL16 can directly bind to DRG neurons via CXCR6. These findings support
319 our premise that CXCL16 can induce knee hyperalgesia through direct binding to CXCR6+
320 nociceptive neurons. Of note, Wang, et. al did not empirically test whether CXCL16 operates via
321 CXCR6, and our study did not measure CXCR6 expression by joint-resident nociceptors, which
322 is an important future direction. However, using a small-molecule CXCR6 antagonist, we
323 confirmed the receptor mechanism of CXCL16-induced effects in cultured DRG neurons *in vitro*
324 and in CXCL16-induced joint hyperalgesia *in vivo,* providing the first mechanistic evidence for a
325 CXCL16-CXCR6 binding interaction that promotes peripheral nociceptive signaling and pain-
326 related behaviors.

327 CXCL16 has been shown to induce calcium mobilization in a CXCR6-expressing murine
328 pre-B lymphoma cell line(*17*) and previous studies in rat and mouse DRGs have established the
329 direct activation of Ca^{2+} mobilization by other chemokines, including CCL2/MCP-1,
330 CCL5/RANTES, CXCL1/fractalkine(*30*), and CXCL5(*31*). However, to date, CXCL16 has not
331 been tested in this context. Our studies advance the understanding of the role of CXCL16-
332 CXCR6 in calcium mobilization, as we demonstrated that CXCL16 can directly stimulate
333 calcium signaling in mouse DRG neurons via CXCR6. Although a direct connection between
334 CXCL16-CXCR6 and pain-related behaviors has not previously been established, CXCL16 has
335 been connected to the nervous system through roles in neurotransmitter release and neuronal-
336 glial cellular crosstalk(*41–43*). CXCL16 and CXCR6 have been shown to be expressed by
337 astrocytes, microglia, and neurons in hippocampal cultures, indicating a potential for CXCL16-
338 CXCR6 signaling(*42*). Di Castro, et. al, observed that CXCL16 promotes spontaneous GABA
339 release in pyramidal neurons from the hippocampal CA1 area(*41*). Wang, et al. also showed that
340 CXCL16 worked synergistically with norepinephrine to increase DRG hyperexcitability and
341 exacerbate neuropathic pain(*40*). Our finding that CXCL16 induces acute knee hyperalgesia, as
342 early as 30 minutes post-injection, suggests that CXCL16 is interacting directly with intra-
343 articular nociceptors, but further studies are required to determine whether this hypothesized
344 activation is due to modulation of Ca^{2+} influx, neurotransmitter release, or some other
345 mechanism.

346 CXCL16 and CXCR6 have been established as inflammatory markers across multiple
347 diseases including high-grade prostate cancer, which is considered an inflammation associated

348 cancer(*44*). Lehrke, et. al., also suggest a pro-inflammatory role for CXCL16 in inflammatory
349 bowel disease as CXCL16 was highly enriched in patients with Crohn's disease or ulcerative
350 colitis and the elevated CXCL16 levels correlated with level of C-reactive protein(*45*). Our
351 studies also demonstrate a pro-inflammatory role for CXCL16, showing that CXCL16 elicits a
352 pro-inflammatory response in synovium *in vivo* and in fibroblasts and macrophages *in vitro*.
353 However, these responses were not tested alongside the CXCR6 antagonist ML339, and thus we
354 cannot conclude whether pro-inflammatory effects were mediated by CXCR6. Further, we
355 demonstrate mitigated CXCL16-induced pain following co-administration with ML339 in a
356 repeated injection experimental design, but we did not evaluate whether co-administration with
357 ML339 also mitigated the pro-inflammatory activation of the synovium that was observed in
358 males. Future studies aim to address these limitations. In a cardiotoxin injection model of muscle
359 injury, CXCL16 knockout mice had decreased macrophage infiltration but increased neutrophil
360 infiltration to injured muscle as compared to controls(*46*). CXCL16 knockout mice also had
361 decreased infiltration of Ly6C^{hi} monocytes and macrophages in the infarcted heart following
362 myocardial infarction(*47*). These studies and our data support the function of CXCL16 as a
363 macrophage chemoattractant across multiple tissue types, and our findings extend this
364 knowledge by demonstrating its pro-inflammatory effects in synovial fibroblasts.

365 To the author's knowledge, while the CXCR6 antagonist ML339 has been validated *in*
366 *vitro*(*48*), *in vivo* use has been limited to a few cancer studies(*49*, *50*) and no study to date has
367 used ML339 *in vivo* under any musculoskeletal health context. While systemic administration of
368 the CXCR6 antagonist acutely ablated joint injury-induced hyperalgesia, it did not mitigate
369 overall hyperalgesia development via disease modification at 7d post-ACLR. These findings
370 indicate that the development of joint hyperalgesia following injury is not solely dependent upon
371 CXCR6, but that CXCL16-CXCR6 at least partially mediate acute nociception. As CXCL16 is
372 the only described ligand for CXCR6, we conclude that the injury-induced upregulation of
373 CXCL16 in the joint, which we confirmed at the protein level in synovial fluid, is partially
374 responsible for injury-induced hyperalgesia, which can be transiently blocked by targeting the
375 CXCR6 receptor. The notion of synovium-derived CXCL16 ligand inducing knee hyperalgesia
376 by binding to intra-articular nociceptors is supported by a meta-analysis of human osteoarthritic
377 synovium. Newton, et. al, unbiasedly identified a putative synovium-DRG interactome focused

378 on neuro-immune/neuro-inflammatory pathways, of which synovium-derived CXCL16 was
379 predicted to interact with nociceptor-bound CXCR6(*51*).

380 Our findings should be interpreted in light of several limitations. The sex-specific
381 differences in the synovial transcriptome and acute hyperalgesia observed in response to intra-
382 articular CXCL16 injection highlight an area needing further investigation. Such studies should
383 address whether this is related to a dose dependency. This will allow future refinement of
384 treatment approaches that account for sex as a biological variable. Furthermore, the efficiency of
385 *in vivo* CXCR6 antagonism by ML339 is unclear, and residual CXCR6-mediated signaling by
386 incomplete receptor inhibition may compensate certain responses, which should be addressed by
387 studies employing genetic knockouts of CXCL16 and CXCR6. The magnitude of contribution of
388 direct CXCL16 binding to intra-articular nociceptors versus secondary stimulation of nociceptors
389 via CXCL16-driven immune cell activation to *in vivo* CXCL16-dependent pain regulation
390 requires further investigation. While our study provides a comprehensive examination of the role
391 of CXCL16 within murine models, there is a need to validate these findings in larger animal
392 models, and human synovial cells and DRGs. Moreover, our study focused mainly on the acute
393 phases of PTOA, with limited assessments of the long-term effects of CXCL16 activation or
394 CXCR6 inhibition. Chronic pain and progressive joint degeneration are characteristic of PTOA,
395 and thus longer-term studies are needed to understand whether the analgesic effects of CXCR6
396 inhibition are sustained throughout PTOA progression.

397 In summary, our study unveils the CXCL16-CXCR6 axis as a novel mediator of joint
398 inflammation and nociception in PTOA while also establishing pharmacological CXCR6
399 antagonism as a potential therapeutic strategy to treat joint trauma-related inflammation and
400 pain.

401 **MATERIALS AND METHODS:**

402 *Study design*

403 The objectives of this study were to: 1) Evaluate the CXCL16 signaling axis in the
404 context of PTOA; 2) establish key mediators and downstream effectors of CXCL16; 3) identify
405 the sufficiency of CXCL16 in driving synovial inflammation and joint nociception, and finally,
406 4) establish a receptor mechanism through which CXCL16 exerts its effects. To explore how

407 CXCL16 expression is altered following murine joint injury and in human OA synovium, we
408 mined bulk and single cell RNAseq datasets and RNA microarrays from mouse and human
409 synovium. Flow cytometry was used to identify CXCL16+ and CXCR6+ cells in healthy and
410 injured mouse synovium, and ELISA was used to measure CXCL16 protein in synovial fluid. *In*
411 *vitro* studies examined the effects of pro-inflammatory cytokines and CXCL16 treatment in
412 murine joint-relevant cell types. The sufficiency of CXCL16 to induce synovial inflammation
413 and joint nociception *in vivo* was evaluated by repeated joint injections with recombinant
414 CXCL16 in naïve mice, followed by knee hyperalgesia testing, histological evaluation, and bulk
415 RNA sequencing of synovium. The receptor mechanism by which repeated intra-articular dosing
416 of CXCL16 induces knee hyperalgesia was assessed by co-administration of CXCL16 and a
417 CXCR6 antagonist, ML339. To demonstrate whether CXCL16 was directly agonizing
418 nociceptors to induce pain, mice were administered a single intra-articular injection of CXCL16
419 followed by hyperalgesia measurements as early as 30 mins post-injection. This was repeated
420 with co-administration of ML339 to establish CXCR6 as the receptor mediating this effect. The
421 role of CXCL16 in driving joint injury-induced pain was tested by administering multiple intra-
422 peritoneal doses of ML339 following noninvasive joint injury in mice and performing knee
423 hyperalgesia assessments longitudinally. Finally, to assess whether CXCL16 can directly activate
424 calcium signaling in nociceptive neurons, we performed *in vitro* calcium imaging of primary
425 DRG-derived neurons from $Na_V1.8$-Cre; $GCaMP6s^{fl/+}$ mice following treatment with CXCL16,
426 with or without CXCR6 antagonist co-treatment. Mice were randomly assigned to groups within
427 an experiment. A blinded operator performed all knee hyperalgesia testing and histopathologic
428 scoring. Sample sizes are detailed in the figure caption and statistical analyses are described in
429 the *Data analysis and statistics* methods section.

430 *Animals and noninvasive ACL rupture*

431 All animal studies were approved by the institutional animal care and use committee.
432 Male and female C57BL/6 mice aged 12-15 weeks (Jackson Laboratories) were used throughout.
433 To induce joint injury and PTOA, we employed a noninvasive mechanical loading-based anterior
434 cruciate ligament rupture (ACLR) model(*32*, *36*) (**Suppl. Materials and Methods**). Limbs from
435 either Sham mice (no loading, with anesthesia and analgesia only) or unloaded contralateral
436 limbs from injured mice served as controls. Naïve male and female $Na_V1.8$-Cre; $GCaMP6s^{fl/+}$

437 mice(*39*) older than 12 weeks were used to obtain primary DRG cultures for *in vitro* Ca^{2+}
438 imaging experiments.

439 *Bulk RNA sequencing, single-cell RNA-sequencing, RNA microarray published data mining*

440 Existing, published bulk RNAseq data generated by our group(*32*) was re-analyzed to
441 assess injury-induced gene expression of all CCL and CXCL family chemokines and their
442 receptors in Sham, ACLR 7d, and ACLR 28d male and female synovia (**Suppl. Materials and**
443 **Methods**).

444 To assess expression patterns of Cxcl16, Cxcr6, and Adam10 in synovium, existing
445 published scRNAseq data from mouse and human OA synovium was analyzed using R. Mouse
446 scRNAseq previously published in our lab(*35*) was mined to examine synovial cell types
447 expressing *Cxcl16*, *Cxcr6*, and *Adam10*. Feature plots showing the expression of the genes of
448 interest across the all cells object, which contains integrated Sham, 7d ACLR, and 28d ACLR
449 synovial cells were generated using the *Shiny* R package.

450 A meta-analysis of human OA synovium bulk RNAseq and RNA microarray datasets
451 was performed using weighted Limma-Voom. Data from these is given as $\log_2$(fold change) and
452 -log10(P_{adj}). Unadjusted *P*-values from individual studies were combined across datasets into a
453 composite *P*-value using the weighted *Z*-test, with a BH (e.g. FDR) correction for multiple
454 comparisons applied following combination. This test is directional, so a positive change in one
455 study and negative change in another cancel out rather than combining. Composite data is
456 presented only as a signed $-\log_{10}(P_{adj})$, since $\log_2$(fold change) cannot be validly combined
457 between RNAseq and RNA microarray datasets. For genes which were missing from some
458 microarrays, only datasets which contained these genes were included in the composite *P*-value
459 calculation.

460 *Synovial fluid collection and protein quantification*

461 Synovial fluid was collected from joints as previously described(*36, 52*). In brief,
462 following euthanasia, a small, consistently-sized alginate sponge was inserted into the joint space
463 through a small incision made in the suprapatellar capsule. Synovial fluid-soaked sponges were
464 flash frozen and stored at -80C. Following thawing, sponges were digested via alginate lyase,
465 and digestates were assayed for CXCL16 content by ELISA (Invitrogen: EMCXCL16). Total

466 protein was quantified in the same samples via Pierce™ Bradford Plus Protein Assay Kit
467 (ThermoFisher Scientific, Cat. #23236). CXCL16 concentrations were normalized to total
468 protein.

469 *Flow cytometry*

470 Whole synovium, inclusive of Hoffa's fat pad, was dissected and enzymatically digested
471 to yield single-cell suspensions using Liberase TM, Collagenase IV, and DNaseI(*35*, *36*). Each
472 sample consisted of one male and one female synovium pooled at the time of dissection (n=3
473 ACLR, n=3 contralateral). After digestion, single cell suspensions were stained (**Suppl.**
474 **Materials and Methods**). Flow cytometry was performed on a BD LSRFortessa and analysis
475 was performed in FlowJo v10 software (BD/TreeStar).

476 *Tissue gene expression via RT-qPCR*

477 Dissected joint tissue were homogenized in TRIzol, RNA was isolated, and qPCR was
478 performed to evaluate the expression of target genes (**Suppl. Materials and Methods**). Data was
479 normalized to housekeeping genes and reported further normalized to experimental controls
480 using the $2^{-\Delta\Delta CT}$ method.

481 *Primary cell isolation and in vitro treatments*

482 Primary fibroblast-like synoviocytes (FLS) from knee synovia, bone marrow-derived
483 macrophages (BMDMs), and bone marrow-derived mesenchymal progenitor cells (BMPCs)
484 were isolated from naïve adult male and female C57BL/6 mice, as previously described(*35*)
485 (**Suppl. Materials and Methods).**

486 To ascertain upstream activators of *Cxcl16* and related gene expression, FLS, BMDMs,
487 and BMPCs were treated with PBS (control), TNF-α (10 ng/mL), or IL-1β (10 ng/mL) for 48
488 hours (FLS, BMPCs) or 8 hours (BMDMs) and then harvested and processed for RT-qPCR.
489 Conditioned media from FLS was also collected for CXCL16 protein quantification via ELISA.
490 To assess the potential functional role of CXCL16, FLS, BMDMs, and BMPCs were treated with
491 PBS (control) or CXCL16 (10ng/mL or 50 ng/mL) for 48 hours (FLS, BMPCs) or 8 hours
492 (BMDMs) and then harvested and processed for RT-qPCR. All *in vitro* experiments were

493 conducted in n=4-8 biological replicates, i.e. cell isolations from unique mice (**Suppl. Materials**
494 **and Methods)**.

495 *ATDC5 cell culture*

496 Following differentiation (**Suppl. Materials and Methods**), chondrogenic ATDC5s were
497 treated with PBS (control), TNF-α (10 ng/mL), or IL-1β (10 ng/mL) for 48 hours, followed by
498 gene expression studies. Briefly, ATDC5s were lysed with Trizol and frozen at -80°C until RNA
499 isolation and gene expression studies by RT-qPCR. All experiments were performed in n=4
500 replicates.

501 *In vitro chemotaxis of BMDMs and BMPCs*

502 BMDMs and BMPCs were separately seeded into transwell insert membranes and
503 combined with a transwell chamber containing either media with vehicle, a positive control (LPS
504 for BMDMs, 5% FBS for BMPCs), or recombinant mouse CXCL16 (10 ng/mL or 50 ng/mL).
505 Cells were allowed to migrate for three days prior to quantification of migrated cell density
506 (**Suppl. Materials and Methods**).

507 *Intraarticular and systemic treatments*

508 Joint injections were administered to the knees of naïve C57Bl/6 mice. All injections
509 were performed using 33G needles and microsyringes (Hamilton Company). To assess the
510 disease-promoting effects of CXCL16 in healthy joints, CXCL16 (R&D Systems, Cat. #503-CX)
511 (0.25 ng or 25 ng in 4 μL of sterile PBS) was injected for five consecutive days into one knee
512 joint, and vehicle was injected in the contralateral joint (n=3 male, n=3 female per dose). Knee
513 hyperalgesia testing occurred at 7d and 14d post-first injection. At 14d post-first injection
514 hindlimbs were harvested for histological evaluation of PTOA and synovitis severity. A separate
515 group of mice (n=3 male, n= 3 female) underwent a similar regiment of 5 consecutive intra-
516 articular injections of CXCL16 into one knee joint (25 ng in 4 μL of sterile PBS with .1% BSA)
517 and vehicle (sterile PBS with .1% BSA) into the contralateral. A baseline measurement of knee
518 hyperalgesia was taken pre-injection then knee hyperalgesia and synovial harvests for bulk RNA
519 sequencing occurred 7d post-first injection. In another cohort, mice received 5 consecutive days
520 of bilateral intra-articular injections of either vehicle (sterile PBS with 0.69% DMSO), CXCL16
521 (200 ng in 5 μL sterile PBS with 0.69% DMSO), or CXCL16 co-administered with CXCR6

522 antagonist, ML339 (MedChemExpress, Cat. #HY-122197) (200 ng CXCL16 in 5 μL sterile PBS
523 with 1mM ML339 and 0.69% DMSO). Knee hyperalgesia was performed at baseline and 7d
524 post-first injection (n=6 males/group).

525 For the first acute hyperalgesia experiment in naïve mice, mice received either a single
526 CXCL16 (25 ng in 4 μL of sterile PBS with 0.1% BSA) or vehicle (sterile PBS with 0.1% BSA)
527 injection into a single joint (n=3 male, n=3 female). Knee hyperalgesia occurred at baseline and
528 30 min, 2 hr, 4 hr, 24 hr, and 7d post-injection (**Fig. 5A**). Mice were divided into two groups for
529 the second acute hyperalgesia experiment in naïve mice (n=9 males/group). One group received
530 an intra-articular injection of CXCL16 (250 ng in 6 μL sterile PBS containing 0.08% BSA and
531 0.69% DMSO) in one knee and vehicle (sterile PBS containing 0.08% BSA, and 0.69% DMSO)
532 in the contralateral. The other group received an intra-articular injection of CXCL16 co-
533 administered with CXCR6 antagonist, ML339, (250 ng CXCL16 in 6 μL sterile PBS containing
534 1mM ML339, 0.08% BSA, and 0.69% DMSO) in one knee and vehicle (sterile PBS containing
535 0.08% BSA, and 0.69% DMSO) in the contralateral. Knee hyperalgesia occurred at baseline and
536 30 min, 2 hr, 4 hr, and 24 hr (**Fig. 5D**). To assess whether ML339 mitigates ACLR-induced
537 effects, injured mice (n=9 males/group) received repeated intraperitoneal injections of either
538 vehicle (corn oil containing 1% DMSO) or ML339 (5 mg/kg of 1.45 mM ML339 in corn oil
539 containing 1% DMSO). Knee hyperalgesia occurred at baseline, 7d post-ACLR prior to
540 injection, and 7d post-ACLR at 2 hrs post-injection (**Fig. 5G**). All mice were randomly assigned
541 to treatment groups within each experiment.

542 *Knee hyperalgesia testing*

543 Knee hyperalgesia testing was performed by a blinded operator (LL) using a Randall-
544 Selitto device as described previously(*32*, *36*). Briefly, pressure was applied to the medial aspect
545 of the knee and the knee withdrawal threshold was recorded when the mouse gave a response – a
546 struggle or vocalization. Three measurements were recorded for each limb and averaged together
547 to obtain the knee withdrawal threshold per limb.

548 *Histological analysis*

549 Whole hindlimbs were processed, stained with Safranin O/Fast Green (SafO), imaged
550 (**Suppl. Materials and Methods**), and qualitatively graded for OA and synovitis severity using

updated and extended versions (**Table S3-S4**) of an established grading scheme(*53, 54*). All grading was performed in a blinded fashion (LL). Scores were averaged across all slides to calculate a limb average, and limbs were averaged to calculate group scores.

Bulk RNA-sequencing and bioinformatic analysis

RNA was isolated from Trizol homogenates of whole synovium, inclusive of Hoffa's fat pad, then sequenced and quality control was performed (**Data file S1**). All Bulk RNA-sequencing data analysis including quality control, gene expression analysis, and pathway analysis was performed in RStudio (R v4.4.0, RStudio v2024.04.1). Differential gene expression analysis was performed using DESeq2(*55*). Pathway analysis was performed using the *clusterProfiler*(*56*) implementation of fast gene set enrichment analysis (GSEA), using the GO: Biological Processes gene ontology terms list (**Suppl. Materials and Methods**).

Complete blood counts

Complete blood count (CBC) analysis was performed using 50-100 µL of blood, obtained via cardiac puncture at the time of harvest.

Primary DRG neuron culture and Ca^{2+} imaging

Primary DRG cultures were generated from $Na_V1.8$-Cre; $GCaMP6s^{fl/+}$ mice as previously described(*57*). These mice express the fluorescent calcium indicator, GCaMP6s, in nociceptive neurons, marked by expression of the voltage-gated sodium channel 1.8 ($Na_V1.8$). L3-L5 DRGs were collected and pooled from 12 wk-old mice, and male and female cultures were generated separately. Four DRGs were used for every coverslip plated. Cultures were maintained at 37°C, treated with CXCL16 with or without pre-treatment with a CXCR6 antagonist, ML339 (180 µM), and fluorescent imaging was performed with Zeiss Zen software to measure Ca^{2+} signaling (n=2-5 well replicates per sex/treatment) (**Suppl. Materials and Methods**). KCl was used as a positive control.

Fluorescent imaging of the calcium sensor was performed at each step of the stimulations and a Fiji macro was used to create videos for calculating (Ft-Fo) / Fo, termed "ΔF/Fo". Regions of interest (ROIs) were circled around individual neurons in Fiji based on responses to KCl and ΔF/Fo was recorded for each ROI. Graphs for each ROI were created in R or in Python. Each

graph and video file were manually checked to determine responses for each neuron. Neurons that responded to vehicle were excluded from further analysis.

Statistical analysis

SPSS (v27, IBM, Armonk, NY) and Prism 10.0 (Graphpad, San Diego, CA) were used for statistical analyses. Paired t-tests compared contralateral and ACLR groups for synovial fluid ELISA and synovial tissue qPCR and flow cytometry analyses. Ordinary one-way ANOVA with Tukey's multiple comparison evaluated treatment differences for *in vitro* cytokine and CXCL16 treatments. Repeated measures one-way ANOVA was used to analyze *in vitro* chemotaxis experiments. Paired t-tests compared knee hyperalgesia threshold and knee withdrawal threshold ratio between vehicle and CXCL16 injected limbs. Paired t-tests within each dose and across both doses of CXCL16 compared histological parameters between vehicle injected and CXCL16 injected limbs. Two-way ANOVA was used to compare knee withdrawal threshold and knee withdrawal threshold ratio between vehicle, CXCL16, and CXCL16 + ML339 injected limbs at baseline and 7d post-injection (factors: timepoint, group). Linear mixed effects models were used to compare knee withdrawal threshold in acute hyperalgesia experiments (**Suppl. Materials and Methods**). Fisher's exact tests within each sex were used to determine associations between the proportion of cells responsive to CXCL16 or to positive control only, in the presence or absence of ML339. *P* values below 0.05 were considered significant throughout.

List of Supplementary Materials

Materials and Methods

Fig. S1. Synovial gene expression of chemokine ligands and chemokine receptors is perturbed in mouse and human OA.

Fig. S2. qPCR corroboration of CXCL16 signaling axis expression and flow cytometry supplement

Fig. S3. CXCL16 treatment *in vitro* – individual expression of macrophage score genes.

Fig. S4. Acute knee hyperalgesia supplement.

Fig. S5. Bulk RNAseq PCA plot.

606 Table S1. Antibodies.

607 Table S2. Gene primers for qPCR.

608 Table S3. PTOA severity scoring.

609 Table S4. Synovitis severity scoring.

610 Data file S1. Synovial bulk RNA-seq – quality control.

611 Data file S2. Synovial bulk RNA-seq – DEG lists.

612 **References**

613 1. C. R. Scanzello, S. R. Goldring, The role of synovitis in osteoarthritis pathogenesis. *Bone*
614 **51**, 249–257 (2012).

615 2. E. Sanchez-Lopez, R. Coras, A. Torres, N. E. Lane, M. Guma, Synovial inflammation in
616 osteoarthritis progression. *Nat Rev Rheumatol* **18**, 258–275 (2022).

617 3. F. Angelini, P. Widera, A. Mobasheri, J. Blair, A. Struglics, M. Uebelhoer, Y. Henrotin,
618 A. C. A. Marijnissen, M. Kloppenburg, F. J. Blanco, I. K. Haugen, F. Berenbaum, C.
619 Ladel, J. Larkin, A. C. Bay-Jensen, J. Bacardit, Osteoarthritis endotype discovery via
620 clustering of biochemical marker data. *Ann Rheum Dis* **81**, 666–675 (2022).

621 4. M. F. Rai, K. H. Collins, A. Lang, T. Maerz, J. Geurts, C. Ruiz-Romero, R. K. June, Y.
622 Ramos, S. J. Rice, S. A. Ali, C. Pastrello, I. Jurisica, C. T. Appleton, J. S. Rockel, M.
623 Kapoor, Three decades of advancements in osteoarthritis research: insights from
624 transcriptomic, proteomic, and metabolomic studies. *Osteoarthritis Cartilage* **32**, 385–397
625 (2024).

626 5. J. P. M. Blair, C. Bager, A. Platt, M. Karsdal, A.-C. Bay-Jensen, Identification of
627 pathological RA endotypes using blood-based biomarkers reflecting tissue metabolism. A
628 retrospective and explorative analysis of two phase III RA studies. *PLoS One* **14**,
629 e0219980 (2019).

630 6. S. Ishihara, A. M. Obeidat, D. L. Wokosin, D. Ren, R. J. Miller, A.-M. Malfait, R. E.
631 Miller, The role of intra-articular neuronal CCR2 receptors in knee joint pain associated
632 with experimental osteoarthritis in mice. *Arthritis Res Ther* **23**, 1–12 (2021).

633 7. J. Miotla Zarebska, A. Chanalaris, C. Driscoll, A. Burleigh, R. E. Miller, A. M. Malfait, B.
634 Stott, T. L. Vincent, CCL2 and CCR2 regulate pain-related behaviour and early gene
635 expression in post-traumatic murine osteoarthritis but contribute little to chondropathy.
636 *Osteoarthritis Cartilage* **25**, 406–412 (2017).

637 8. R. E. Miller, P. B. Tran, R. Das, N. Ghoreishi-Haack, D. Ren, R. J. Miller, A.-M. Malfait,
638 CCR2 chemokine receptor signaling mediates pain in experimental osteoarthritis.
639 *Proceedings of the National Academy of Sciences* **109**, 20602–20607 (2012).

640 9. C. T. G. Appleton, S. E. Usmani, M. A. Pest, V. Pitelka, J. S. Mort, F. Beier, Reduction in
641 disease progression by inhibition of transforming growth factor α–CCL2 signaling in
642 experimental posttraumatic osteoarthritis. *Arthritis & rheumatology* **67**, 2691–2701
643 (2015).

644 10. L. Longobardi, J. D. Temple, L. Tagliafierro, H. Willcockson, A. Esposito, N. D'Onofrio,
645 E. Stein, T. Li, T. J. Myers, H. Ozkan, M. L. Balestrieri, V. Ulici, R. F. Loeser, A.
646 Spagnoli, Role of the CC chemokine receptor-2 in a murine model of injury-induced
647 osteoarthritis. *Osteoarthritis Cartilage* **25**, 914–925 (2017).

648 11. C. Tang, C. Hsu, Y. Fong, The CCL5/CCR5 axis promotes interleukin-6 production in
649 human synovial fibroblasts. *Arthritis Rheum* **62**, 3615–3624 (2010).

650 12. H. Raghu, C. M. Lepus, Q. Wang, H. H. Wong, N. Lingampalli, F. Oliviero, L. Punzi, N.
651 J. Giori, S. B. Goodman, C. R. Chu, J. B. Sokolove, W. H. Robinson, CCL2/CCR2, but
652 not CCL5/CCR5, mediates monocyte recruitment, inflammation and cartilage destruction
653 in osteoarthritis. *Ann Rheum Dis* **76**, 914–922 (2017).

654 13. S. Abel, C. Hundhausen, R. Mentlein, A. Schulte, T. A. Berkhout, N. Broadway, D.
655 Hartmann, R. Sedlacek, S. Dietrich, B. Muetze, B. Schuster, K. J. Kallen, P. Saftig, S.
656 Rose-John, A. Ludwig, The transmembrane CXC-chemokine ligand 16 is induced by IFN-
657 gamma and TNF-alpha and shed by the activity of the disintegrin-like metalloproteinase
658 ADAM10. *J Immunol* **172**, 6362–6372 (2004).

659 14. T. Nakayama, K. Hieshima, D. Izawa, Y. Tatsumi, A. Kanamaru, O. Yoshie, Cutting
660 edge: profile of chemokine receptor expression on human plasma cells accounts for their
661 efficient recruitment to target tissues. *The Journal of Immunology* **170**, 1136–1140 (2003).

662 15. K. Hattermann, K. Bartsch, H. H. Gebhardt, H. M. Mehdorn, M. Synowitz, A. D. Schmitt,
663 R. Mentlein, J. Held-Feindt, "Inverse signaling" of the transmembrane chemokine
664 CXCL16 contributes to proliferative and anti-apoptotic effects in cultured human
665 meningioma cells. *Cell Communication and Signaling* **14**, 1–11 (2016).

666 16. K. Hattermann, H. Gebhardt, S. Krossa, A. Ludwig, R. Lucius, J. Held-Feindt, R.
667 Mentlein, Transmembrane chemokines act as receptors in a novel mechanism termed
668 inverse signaling. *Elife* **5**, e10820 (2016).

669 17. A. Wilbanks, S. C. Zondlo, K. Murphy, S. Mak, D. Soler, P. Langdon, D. P. Andrew, L.
670 Wu, M. Briskin, Expression cloning of the STRL33/BONZO/TYMSTR ligand reveals
671 elements of CC, CXC, and CX3C chemokines. *The Journal of Immunology* **166**, 5145–
672 5154 (2001).

673 18. M. Matloubian, A. David, S. Engel, J. E. Ryan, J. G. Cyster, A transmembrane CXC
674 chemokine is a ligand for HIV-coreceptor Bonzo. *Nat Immunol* **1**, 298–304 (2000).

675 19. A. N. Wein, S. R. McMaster, S. Takamura, P. R. Dunbar, E. K. Cartwright, S. L.
676 Hayward, D. T. McManus, T. Shimaoka, S. Ueha, T. Tsukui, T. Masumoto, M. Kurachi,
677 K. Matsushima, J. E. Kohlmeier, CXCR6 regulates localization of tissue-resident memory
678 CD8 T cells to the airways. *J Exp Med* **216**, 2748–2762 (2019).

679 20. K. Heesch, F. Raczkowski, V. Schumacher, S. Hunemorder, U. Panzer, H. W. Mittrucker,
680 The function of the chemokine receptor CXCR6 in the T cell response of mice against
681 Listeria monocytogenes. *PLoS One* **9**, e97701 (2014).

682 21. M. J. Butcher, C. I. Wu, T. Waseem, E. V Galkina, CXCR6 regulates the recruitment of
683 pro-inflammatory IL-17A-producing T cells into atherosclerotic aortas. *Int Immunol* **28**,
684 255–261 (2016).

685 22. K. M. Krawczyk, H. Nilsson, R. Allaoui, D. Lindgren, M. Arvidsson, K. Leandersson, M.
686 E. Johansson, Papillary renal cell carcinoma-derived chemerin, IL-8, and CXCL16
687 promote monocyte recruitment and differentiation into foam-cell macrophages. *Lab Invest*
688 **97**, 1296–1305 (2017).

689 23. R. van der Voort, A. W. van Lieshout, L. W. Toonen, A. W. Sloetjes, W. B. van den Berg,
690 C. G. Figdor, T. R. Radstake, G. J. Adema, Elevated CXCL16 expression by synovial
691 macrophages recruits memory T cells into rheumatoid joints. *Arthritis Rheum* **52**, 1381–
692 1391 (2005).

693 24. N. R. Dhoke, K. Kaushik, A. Das, Cxcr6-Based Mesenchymal Stem Cell Gene Therapy
694 Potentiates Skin Regeneration in Murine Diabetic Wounds. *Mol Ther*, doi:
695 10.1016/j.ymthe.2020.02.014 (2020).

696 25. J. H. Ruth, C. S. Haas, C. C. Park, M. A. Amin, R. J. Martinez, G. K. Haines 3rd, S.
697 Shahrara, P. L. Campbell, A. E. Koch, CXCL16-mediated cell recruitment to rheumatoid
698 arthritis synovial tissue and murine lymph nodes is dependent upon the MAPK pathway.
699 *Arthritis Rheum* **54**, 765–778 (2006).

700 26. X. Zhang, J. X. Zhao, L. Sun, X. Y. Liu, [Expression of CXCL16/CXCR6 in fibroblast-
701 like synoviocytes in rheumatoid arthritis and its role in synoviocyte proliferation]. *Beijing*
702 *Da Xue Xue Bao Yi Xue Ban* **49**, 663–668 (2017).

703 27. T. Isozaki, A. S. Arbab, C. S. Haas, M. A. Amin, M. D. Arendt, A. E. Koch, J. H. Ruth,
704 Evidence that CXCL16 is a potent mediator of angiogenesis and is involved in endothelial
705 progenitor cell chemotaxis : studies in mice with K/BxN serum-induced arthritis. *Arthritis*
706 *Rheum* **65**, 1736–1746 (2013).

707 28. T. Nanki, T. Shimaoka, K. Hayashida, K. Taniguchi, S. Yonehara, N. Miyasaka,
708 Pathogenic role of the CXCL16–CXCR6 pathway in rheumatoid arthritis. *Arthritis &*
709 *Rheumatism: Official Journal of the American College of Rheumatology* **52**, 3004–3014
710 (2005).

711 29. R. E. Miller, R. J. Miller, A.-M. Malfait, Osteoarthritis joint pain: the cytokine connection.
712 *Cytokine* **70**, 185–193 (2014).

713 30. S. B. Oh, P. B. Tran, S. E. Gillard, R. W. Hurley, D. L. Hammond, R. J. Miller,
714 Chemokines and glycoprotein120 produce pain hypersensitivity by directly exciting
715 primary nociceptive neurons. *Journal of Neuroscience* **21**, 5027–5035 (2001).

716 31. C. Yin, B. Liu, Z. Dong, S. Shi, C. Peng, Y. Pan, X. Bi, H. Nie, Y. Zhang, Y. Tai, Q. Hu,
717 X. Wang, X. Shao, H. An, J. Fang, C. Wang, B. Liu, CXCL5 activates CXCR2 in
718 nociceptive sensory neurons to drive joint pain and inflammation in experimental gouty
719 arthritis. *Nat Commun* **15**, 3263 (2024).

720 32. R. F. Bergman, L. Lammlin, L. Junginger, E. Farrell, S. Goldman, R. Darcy, C. Rasner, A.
721 M. Obeidat, A.-M. Malfait, R. E. Miller, T. Maerz, Sexual dimorphism of the synovial
722 transcriptome underpins greater PTOA disease severity in male mice following joint
723 injury. *Osteoarthritis Cartilage* **32**, 1060–1073 (2024).

724 33. P. J. Gough, K. J. Garton, P. T. Wille, M. Rychlewski, P. J. Dempsey, E. W. Raines, A
725 disintegrin and metalloproteinase 10-mediated cleavage and shedding regulates the cell
726 surface expression of CXC chemokine ligand 16. *The Journal of Immunology* **172**, 3678–
727 3685 (2004).

728 34. N. Bao, B. Fu, X. Zhong, S. Jia, Z. Ren, H. Wang, W. Wang, H. Shi, J. Li, F. Ge, Q.
729 Chang, Y. Gong, W. Liu, F. Qiu, S. Xu, T. Li, Role of the CXCR6/CXCL16 axis in
730 autoimmune diseases. *Int Immunopharmacol* **121**, 110530 (2023).

731 35. A. J. Knights, E. C. Farrell, O. M. Ellis, L. Lammlin, L. M. Junginger, P. M. Rzeczycki,
732 R. F. Bergman, R. Pervez, M. Cruz, E. Knight, D. Farmer, A. A. Samani, C.-L. Wu, K. D.
733 Hankenson, T. Maerz, Synovial fibroblasts assume distinct functional identities and
734 secrete R-spondin 2 in osteoarthritis. *Ann Rheum Dis* **82**, 272–282 (2023).

735 36. P. Rzeczycki, C. Rasner, L. Lammlin, L. Junginger, S. Goldman, R. Bergman, S. Redding,
736 A. J. Knights, M. Elliott, T. Maerz, Cannabinoid receptor type 2 is upregulated in
737 synovium following joint injury and mediates anti-inflammatory effects in synovial
738 fibroblasts and macrophages. *Osteoarthritis Cartilage* **29**, 1720–1731 (2021).

739 37. R. J. Miller, H. Jung, S. K. Bhangoo, F. A. White, Cytokine and chemokine regulation of
740 sensory neuron function. *Sensory nerves*, 417–449 (2009).

741 38. H.-G. Schaible, Nociceptive neurons detect cytokines in arthritis. *Arthritis Res Ther* **16**, 1–
742 9 (2014).

743 39. A. M. Obeidat, M. J. Wood, N. S. Adamczyk, S. Ishihara, J. Li, L. Wang, D. Ren, D. A.
744 Bennett, R. J. Miller, A.-M. Malfait, R. E. Miller, Piezo2 expressing nociceptors mediate
745 mechanical sensitization in experimental osteoarthritis. *Nat Commun* **14**, 2479 (2023).

746 40. C. Wang, A. Di, Y. Wu, M. Liu, M. Wei, Z. Liang, F. Liu, H. Fan, B. Dong, C. Li,
747 Sprouting sympathetic fibres release CXCL16 and norepinephrine to synergistically
748 mediate sensory neuronal hyperexcitability in a rodent model of neuropathic pain. *Br J*
749 *Anaesth* (2025).

750 41. M. A. Di Castro, F. Trettel, G. Milior, L. Maggi, D. Ragozzino, C. Limatola, The
751 chemokine CXCL16 modulates neurotransmitter release in hippocampal CA1 area. *Sci*
752 *Rep* **6**, 34633 (2016).

753 42. M. Rosito, C. Deflorio, C. Limatola, F. Trettel, CXCL16 orchestrates adenosine A3
754 receptor and MCP-1/CCL2 activity to protect neurons from excitotoxic cell death in the
755 CNS. *Journal of Neuroscience* **32**, 3154–3163 (2012).

756 43. M. Rosito, C. Lauro, G. Chece, A. Porzia, L. Monaco, F. Mainiero, M. Catalano, C.
757 Limatola, F. Trettel, Trasmembrane chemokines CX3CL1 and CXCL16 drive interplay
758 between neurons, microglia and astrocytes to counteract pMCAO and excitotoxic
759 neuronal death. *Front Cell Neurosci* **8**, 193 (2014).

760 44. M. Darash-Yahana, J. W. Gillespie, S. M. Hewitt, Y.-Y. K. Chen, S. Maeda, I. Stein, S. P.
761 Singh, R. B. Bedolla, A. Peled, D. A. Troyer, E. Pikarsky, M. Karin, J. M. Farber, The
762 chemokine CXCL16 and its receptor, CXCR6, as markers and promoters of inflammation-
763 associated cancers. *PLoS One* **4**, e6695 (2009).

764 45. M. Lehrke, A. Konrad, M. Lehrke, A. Konrad, V. Schachinger, C. Tillack, F. Seibold, R.
765 Stark, K. G. Parhofer, U. C. Broedl, CXCL16 is a surrogate marker of inflammatory
766 bowel disease. *Scand J Gastroenterol* **43**, 283–288 (2008).

767 46. L. Zhang, L. Ran, G. E. Garcia, X. H. Wang, S. Han, J. Du, W. E. Mitch, Chemokine
768 CXCL16 regulates neutrophil and macrophage infiltration into injured muscle, promoting
769 muscle regeneration. *Am J Pathol* **175**, 2518–2527 (2009).

770 47. J. Zhang, W. Hao, J. Zhang, T. Li, Y. Ma, Y. Wang, X. Li, W. Cui, J. Du, CXCL16
771 promotes Ly6Chigh monocyte infiltration and impairs heart function after acute
772 myocardial infarction. *The Journal of Immunology* **210**, 820–831 (2023).

773 48. P. M. Hershberger, S. Peddibhotla, E. Sugarman, P. Maloney, D. Key, E. Suyama, K.
774 Nguyen, S. Vasile, M. Kraft, D. Stonich, Probing the CXCR6/CXCL16 axis: targeting
775 prevention of prostate cancer metastasis. *Probe Reports from the NIH Molecular Libraries*
776 *Program [Internet]* (2014).

777 49. S. Peddibhotla, P. M. Hershberger, R. J. Kirby, E. Sugarman, P. R. Maloney, E. H.
778 Sessions, D. Divlianska, C. J. Morfa, D. Terry, A. B. Pinkerton, L. H. Smith, S. Malany,
779 Discovery of small molecule antagonists of chemokine receptor CXCR6 that arrest tumor
780 growth in SK-HEP-1 mouse xenografts as a model of hepatocellular carcinoma. *Bioorg*
781 *Med Chem Lett* **30**, 126899 (2020).

782 50. T. Chen, C. Qiao, E. Yinwang, S. Wang, X. Wen, Y. Feng, X. Jin, S. Li, Y. Xue, H. Zhou,
783 W. Zhang, X. Zeng, Z. Wang, H. Sun, L. Jiang, H. Li, B. Li, Z. Cai, Z. Ye, N. Lin, Natural
784 lung-tropic TH9 cells: a sharp weapon for established lung metastases. *J Immunother*
785 *Cancer* **12**, e009629 (2024).

786 51. M. D. Newton, H. Swahn, D. E. Orange, J. B. Lesnak, T. J. Price, A. M. Malfait, R. E.
787 Miller, M. K. Lotz, T. Maerz, Cross-platform transcriptomic data integration identifies an

788 overactive neuro-immune signature in human osteoarthritis synovium. *Osteoarthritis*
789 *Cartilage*, 1–12 (2025).

790 52. D. R. Seifer, B. D. Furman, F. Guilak, S. A. Olson, S. C. Brooks III, V. B. Kraus, Novel
791 synovial fluid recovery method allows for quantification of a marker of arthritis in mice.
792 *Osteoarthritis Cartilage* **16**, 1532–1538 (2008).

793 53. C. B. Little, A. Barai, D. Burkhardt, S. M. Smith, A. J. Fosang, Z. Werb, M. Shah, E. W.
794 Thompson, Matrix metalloproteinase 13-deficient mice are resistant to osteoarthritic
795 cartilage erosion but not chondrocyte hypertrophy or osteophyte development. *Arthritis*
796 *Rheum* **60**, 3723–3733 (2009).

797 54. M. T. Jackson, B. Moradi, S. Zaki, M. M. Smith, S. McCracken, S. M. Smith, C. J.
798 Jackson, C. B. Little, Depletion of protease-activated receptor 2 but not protease-activated
799 receptor 1 may confer protection against osteoarthritis in mice through extracartilaginous
800 mechanisms. *Arthritis Rheumatol* **66**, 3337–3348 (2014).

801 55. M. I. Love, W. Huber, S. Anders, Moderated estimation of fold change and dispersion for
802 RNA-seq data with DESeq2. *Genome Biol* **15**, 1–21 (2014).

803 56. G. Yu, L.-G. Wang, Y. Han, Q.-Y. He, clusterProfiler: an R package for comparing
804 biological themes among gene clusters. *OMICS* **16**, 284–287 (2012).

805 57. R. E. Miller, S. Ishihara, P. B. Tran, S. B. Golub, K. Last, R. J. Miller, A. J. Fosang, A.-M.
806 Malfait, An aggrecan fragment drives osteoarthritis pain through Toll-like receptor 2. *JCI*
807 *Insight* **3**, e95704 (2018).

808

809 **Acknowledgements:**

810 The authors would like to acknowledge the Michigan Integrative Musculoskeletal Health
811 Core Center (MiMHC) which is supported by P30AR069620 from NIH/NIAMS for processing
812 samples for histology and for use of their microscopy equipment. We also wish to acknowledge
813 the University of Michigan Biomedical Research Core Facilities, specifically the flow cytometry
814 core, which is a part of the Medical School Office of Research, for use of their flow cytometer.
815 We would like to thank the Chicago Center on Musculoskeletal Pain (C-COMP) funded by
816 P30AR079206 for technical assistance with calcium imaging.

Figures and tables:

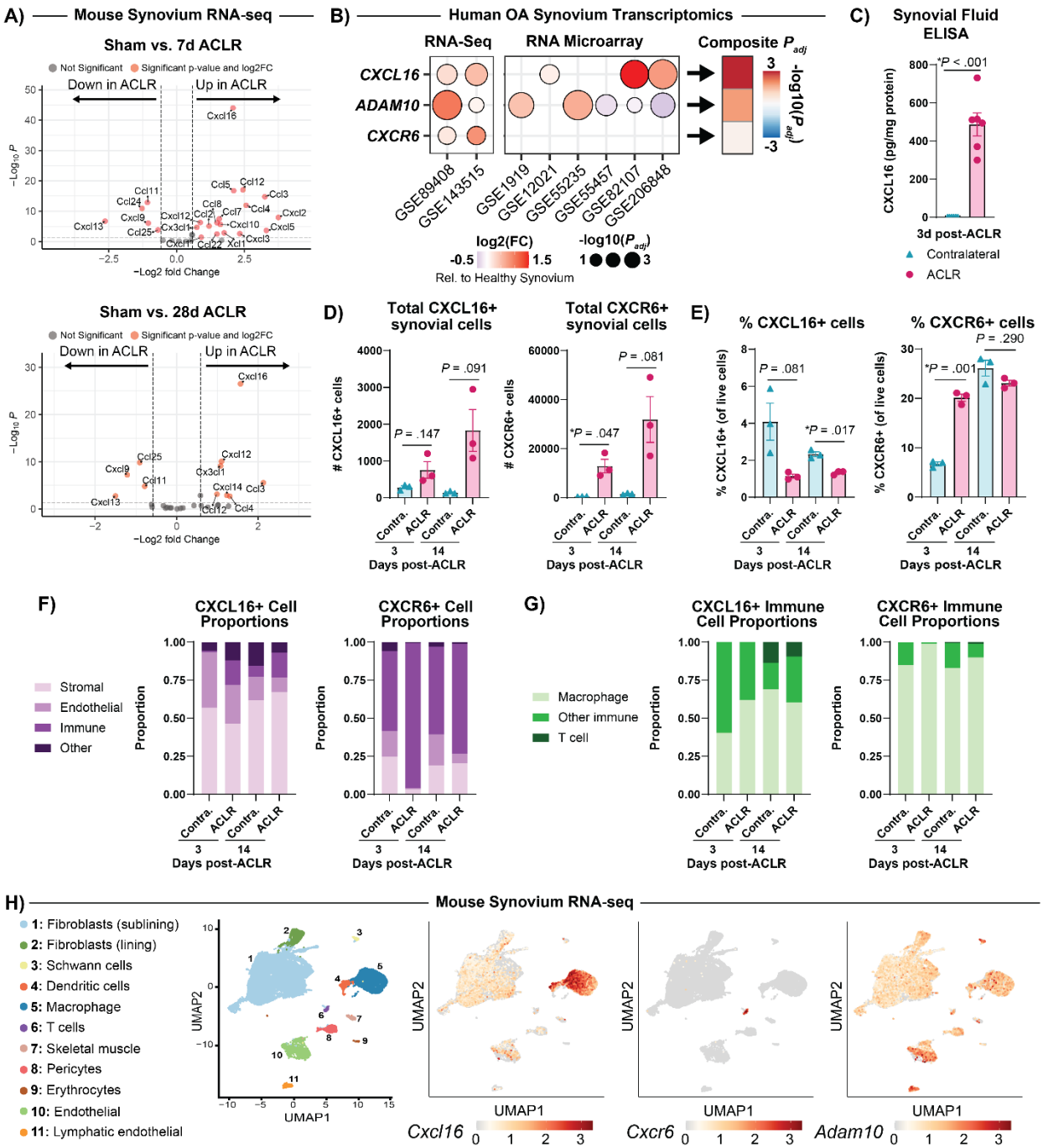

Fig. 1. Joint injury activates the CXCL16-CXCR6 axis in synovium. (**A**) Volcano plots of mouse synovial bulk RNAseq data(*32*) comparing chemokine ligand expression in Sham vs 7d ACLR and Sham vs 28d ACLR. Genes with red datapoints were differentially expressed at $P_{adj} < 0.05$ and $|\log_2 FC| > 0.585$. (**B**) Bubble plot from a meta-analysis of human OA synovial transcriptomics datasets showing expression of *CXCL16*, *CXCR6*, and *ADAM10* relative to

healthy synovium. (**C**) CXCL16 ELISA of synovial fluid in contralateral and injured joints 3d post-ACLR (n=6 per group). Total number of (**D**) and percent positive (**E**) CXCL16+ and CXCR6+ cells in contralateral and injured synovium at 3d and 14d post-ACLR (n=3 per group. 1 sample = 1 male + 1 female synovia pooled). (**F**) Proportions plots showing the cell type breakdown of CXCL16+ and CXCR6+ cells. (**G**) Proportions plots further breaking down the CXCL16+ and CXCR6+ immune cell types. (**H**) Feature plots of mouse synovial single cell RNAseq data(*35*) showing *Cxcl16, Cxcr6,* and *Adam10* gene expression distribution across all cell types. All bars show mean ± SEM.

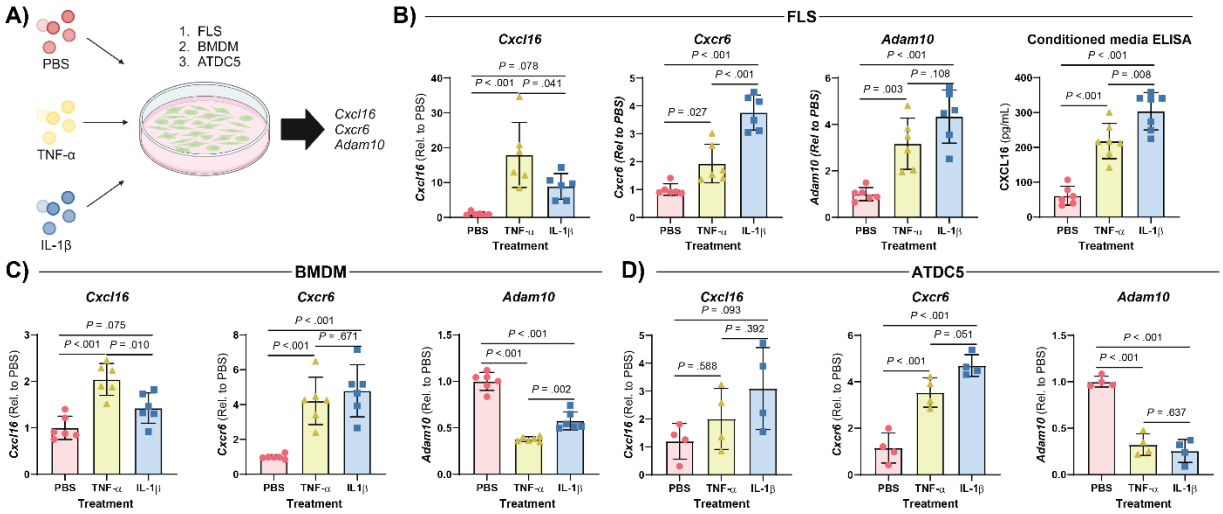

Fig. 2. Upstream mediators of the CXCL16 signaling axis *in vitro.* (**A**) Fibroblast like synoviocytes (FLS), bone marrow-derived macrophages (BMDM), and immortalized chondrogenic cells (ATDC5s) were treated with pro-inflammatory cytokines and perturbation of the CXCL16 signaling axis was evaluated via qPCR. (**B**) Gene expression of *Cxcl16*, *Cxcr6*, and *Adam10* by qPCR in FLS (n=6 per group) and a CXCL16 ELISA of FLS conditioned media (n=6-7 per group). (**C**) Gene expression of *Cxcl16*, *Cxcr6*, and *Adam10* by qPCR in BMDMs (n=6 per group). (**D**) Gene expression of *Cxcl16*, *Cxcr6*, and *Adam10* by qPCR in ATDC5s. (n=4 per group). All bars show mean ± SEM.

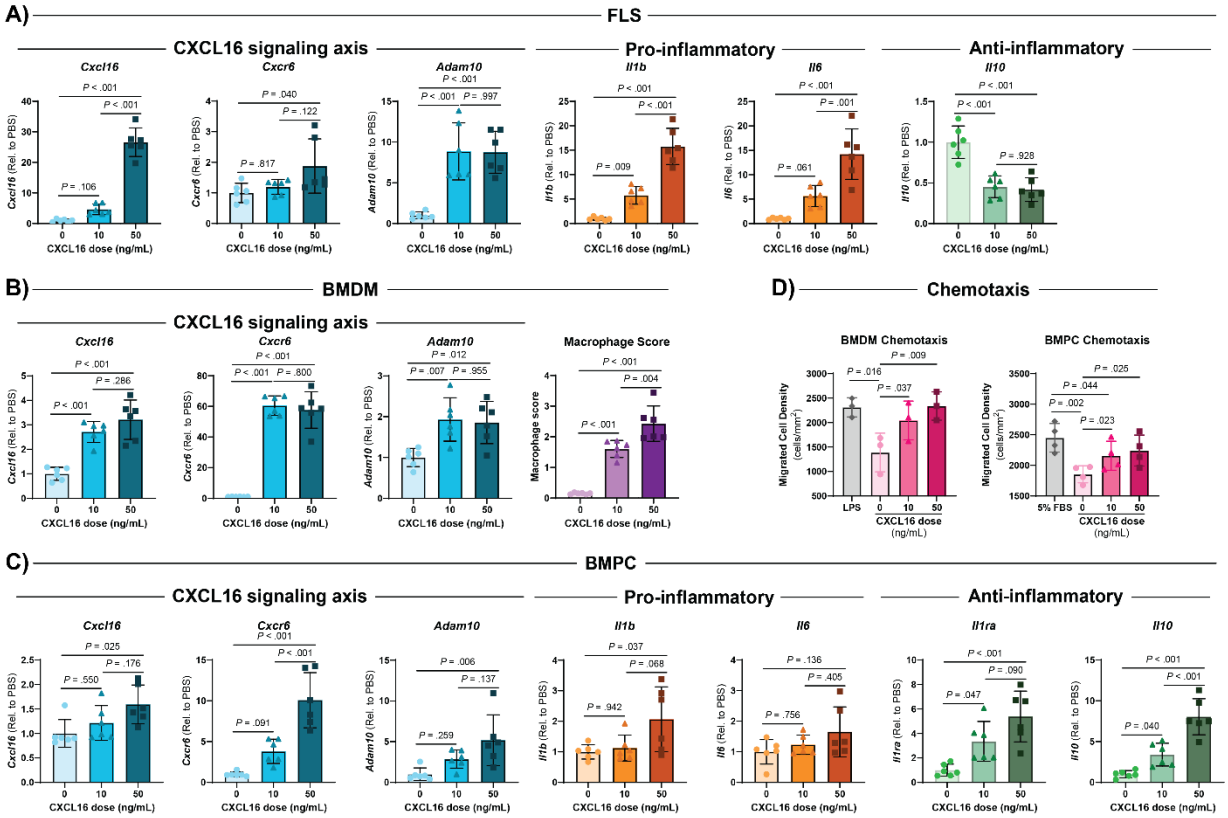

Fig. 3. Downstream effects of CXCL16 *in vitro*. (**A**) In FLS, gene expression of the CXCL16 signaling axis, pro-inflammatory markers, and anti-inflammatory markers was measured by qPCR following stimulation with recombinant CXCL16 (n=6 per group). (**B**) In BMDMs, gene expression of the CXCL16 signaling axis and a macrophage score was measured by qPCR following stimulation with recombinant CXCL16 (n=6 per group). (**C**) In BMPCs, gene expression of the CXCL16 signaling axis, pro-inflammatory markers, and anti-inflammatory markers was measured by qPCR following stimulation with recombinant CXCL16 (n=6 per group). (**D**) Chemotaxis of BMDMs and BMPCs in response to CXCL16 was measured by migrated cell density (n=3 per group). All bars show mean ± SEM.

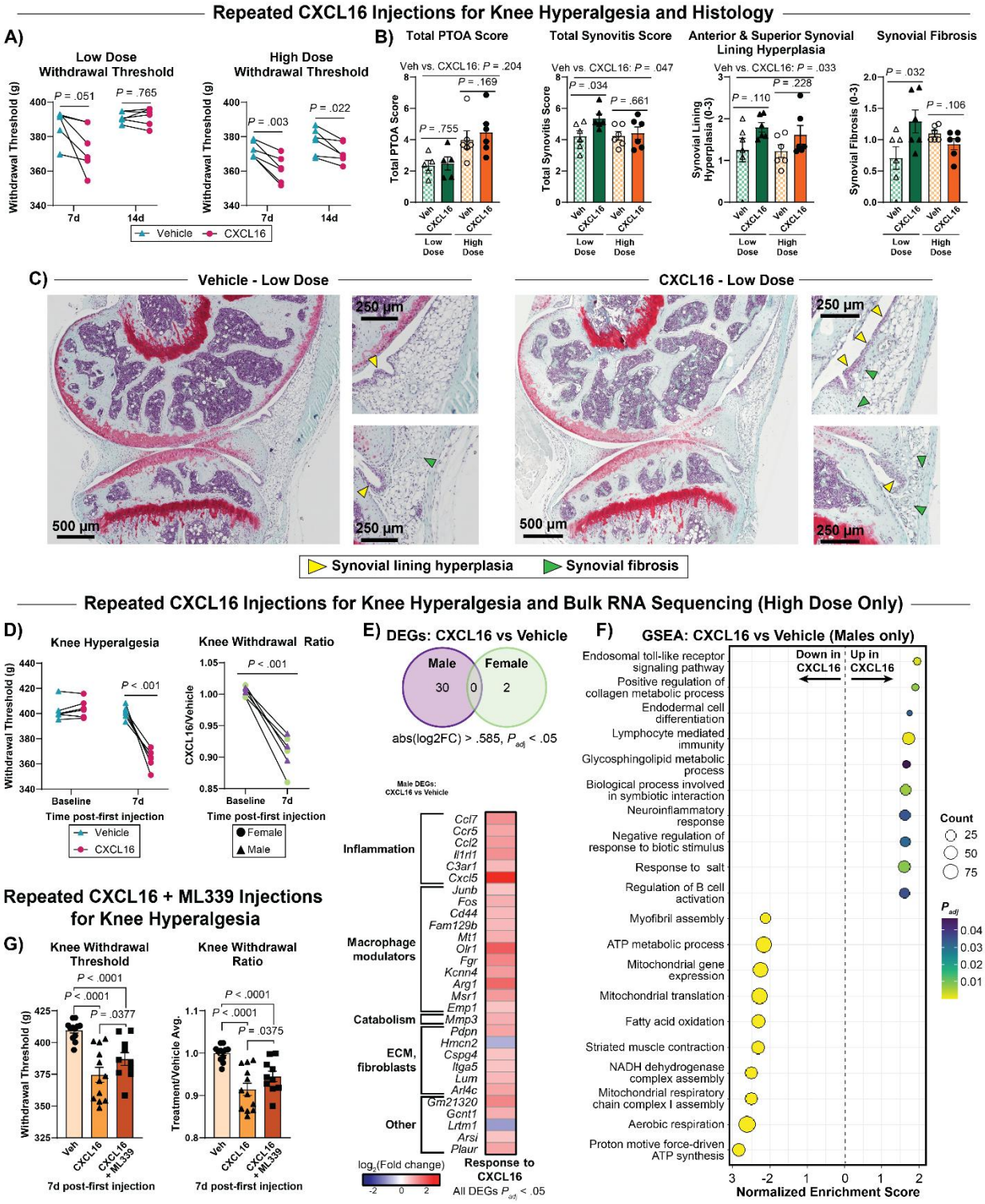

852

853 **Fig. 4. CXCL16-induced hyperalgesia and modulation of the synovial transcriptome.** (**A**)
854 Knee withdrawal threshold following repeated intra-articular injection of CXCL16 (either low
855 dose or high dose) or vehicle in the contralateral side. Testing occurred at 7d and 14d post-first
856 injection (n=6 per dose). (**B**) Histopathological scoring of limbs given repeated intra-articular

857 injections of CXCL16 (either low or high dose) or vehicle in the contralateral side. Total PTOA
858 score and total synovitis score are shown along with the synovitis subscores of anterior, inferior
859 synovial lining hyperplasia and synovial fibrosis (n=5-6 mice per dose, n=3-12 images averaged
860 together per limb). (**C**) Representative low dose CXCL16-injected limbs and vehicle-injected
861 contralateral limbs. Yellow arrows – synovial lining hyperplasia. Green arrows – synovial
862 fibrosis. (**D**) Knee withdrawal threshold and knee withdrawal threshold ratio (CXCL16/vehicle)
863 following repeated intra-articular injection of CXCL16 (high dose only) or vehicle in the
864 contralateral side (n=3 per sex). (**E**) Venn diagram of synovial bulk RNAseq showing
865 differentially expressed genes (DEGs) between vehicle and CXCL16 injected joints in males
866 compared to females (n=3 per group per sex, $|\log_2 FC| > .585$, $P_{adj} < .05$). Heatmap of male
867 DEGs. Red indicates upregulated and blue indicates downregulated in CXCL16 injected joints
868 relative to vehicle injected joints. (**F**) Gene set enrichment analysis of male synovia comparing
869 vehicle vs CXCL16 injected joints. (**G**) Knee withdrawal threshold following repeated bilateral
870 intra-articular injections of vehicle, CXCL16, or CXCL16 co-administered with ML339 (n=6
871 mice, i.e. n=12 limbs, per group). All bars show mean ± SEM.

872

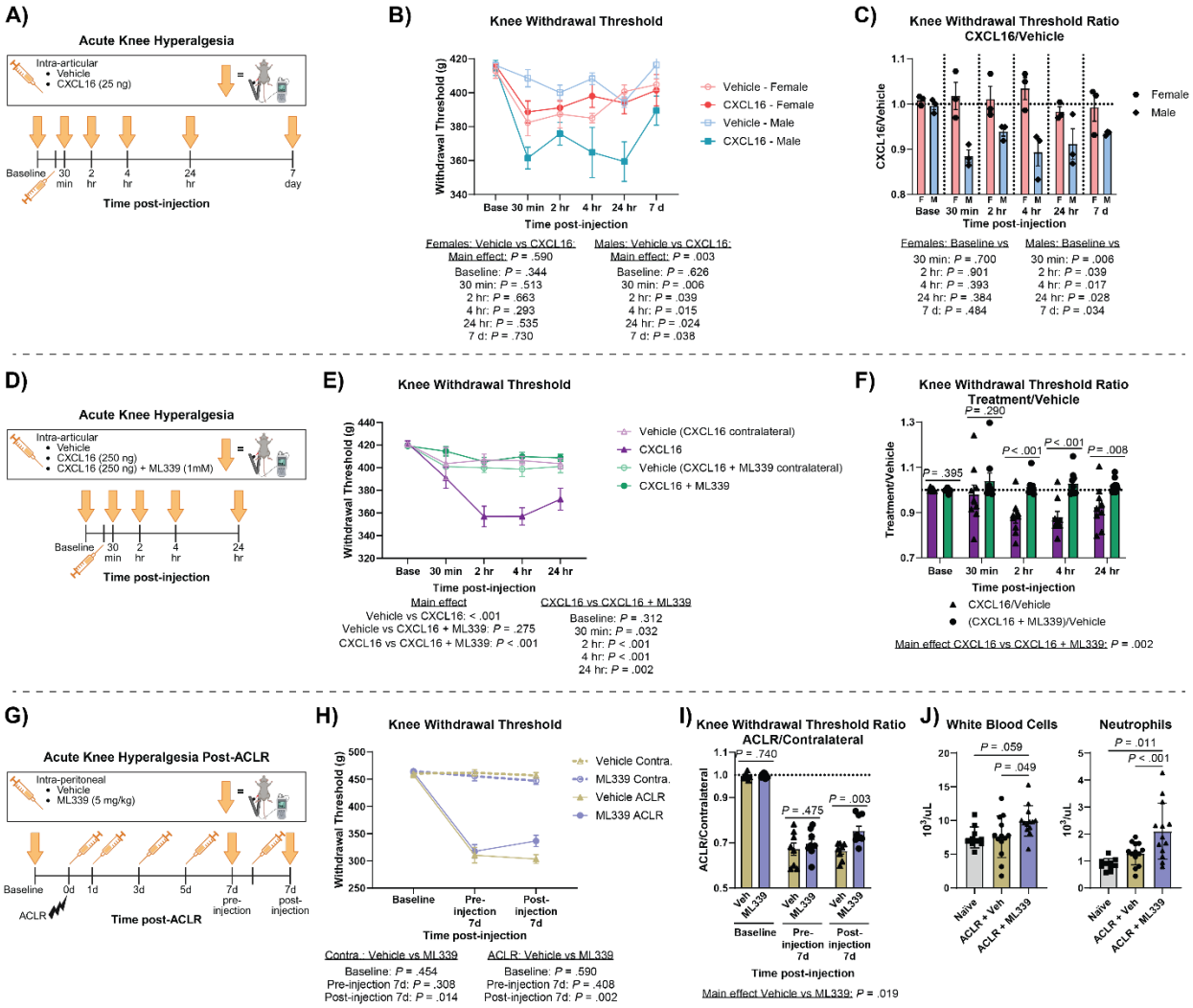

Fig. 5. CXCL16-induced acute hyperalgesia via CXCR6. (**A**) Experimental design for intra-articular CXCL16 injection followed by acute knee hyperalgesia. Knee withdrawal threshold (**B**) and knee withdrawal threshold ratio (**C**) at acute timepoints following intra-articular injection of CXCL16 or vehicle in the contralateral joint (n=3 per sex). (**D**) Experimental design for intra-articular CXCL16 +/- ML339 injection followed by acute knee hyperalgesia. Knee withdrawal threshold (**E**) and knee withdrawal threshold ratio (**F**) at acute timepoints following intra-articular injection of CXCL16 or CXCL16 + ML339, and vehicle in the contralateral joint (n=9 per group). (**G**) Experimental design for intra-peritoneal ML339 injections and acute knee hyperalgesia post-ACLR. Knee withdrawal threshold (**H**) and knee withdrawal threshold ratio (**I**) pre- and post-intraperitoneal injection of vehicle or ML339 at 7d post-ACLR (n=8-9 per group). (**J**) Complete blood count analysis showing total number of circulating white blood cells and

neutrophils from naïve mice and mice treated with vehicle or ML339 7d post-ACLR (n=10-13 per group). All bars show mean ± SEM.

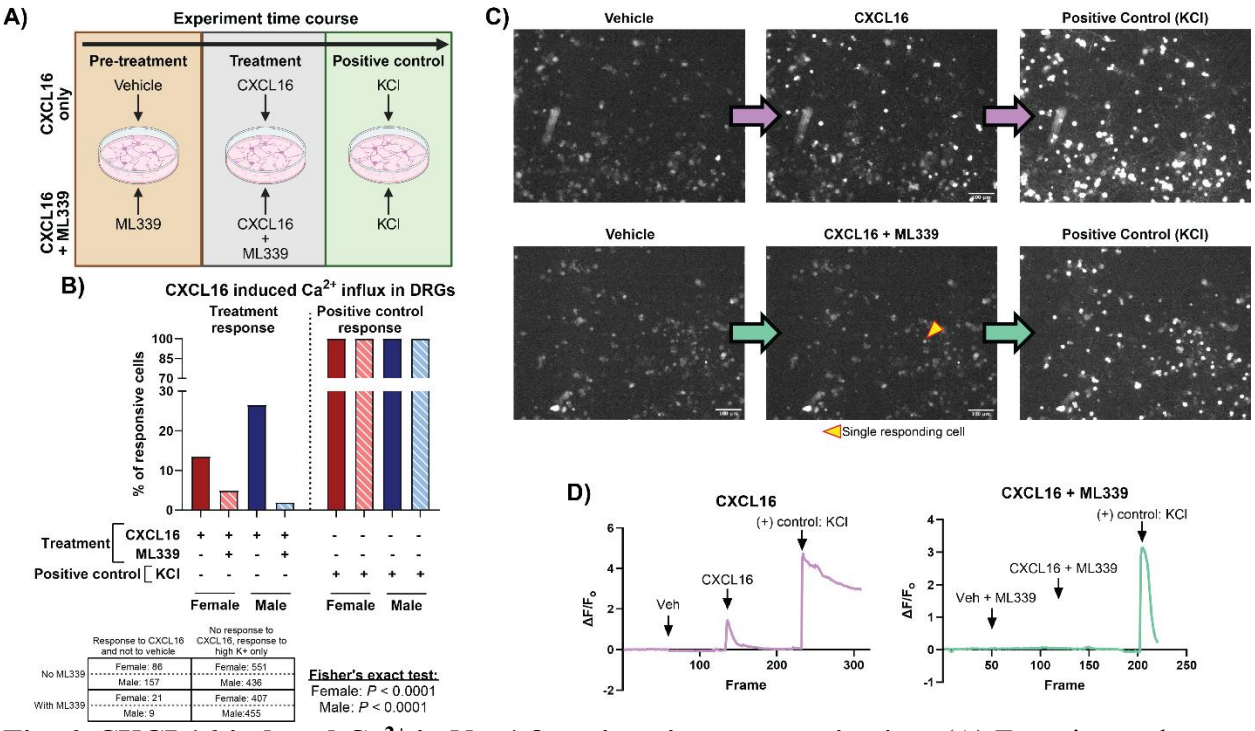

Fig. 6. CXCL16-induced Ca^{2+} in Nav1.8 nociceptive neurons *in vitro*. (**A**) Experimental design: Murine DRG cultures were pre-treated with either vehicle or ML339, treated with CXCL16 or CXCL16 + ML339, and then followed by a positive control stimulus, KCl. (**B**) Quantification of percent responsive cells to CXCL16 stimulation in the presence and absence of CXCR6 antagonist, ML339. Total number of responsive cells is detailed for each sex. (**C**) Representative images of each stage of the experiment – pretreatment, treatment, positive control. (**D**) Representative line plots showing ΔF/Fo of a single responsive cell (responds to KCl) for each condition.

Funding:

National Science Foundation Graduate Research Fellowship grant DGE 2241144 (LL)

National Institutes of Health K99 grant K99AR081894 (AJK)

Pioneer Fellowship from the University of Michigan (AJK)

Orthopaedic Research Society Scientific Network Award (TM, REM)

F31AR083277 (NSA)

R01AR077019 (REM)

R01AR077019-03S1 (REM)

R01AR080035 (TM)

Department of Orthopaedic Surgery, University of Michigan (TM)

Author contributions:

Conceptualization: LL, SR, REM, TM
Methodology: LL, SR, AJK, MDN, PMR, REM, TM
Investigation: LL, SR, AJK, AM, MDN, RFB, IS, SCH, SGN, PMR, NSA
Visualization: LL, AM, MDN, IS
Funding acquisition: LL, NSA, REM, TM
Writing – original draft: LL, TM
Writing – review & editing: LL, AJK, MDN, NSA, REM, TM

Competing interests:

TM is a paid consultant for RelationRx. All other authors declare that they have no competing interests.

Data and materials availability:

Bulk RNA-seq data will be publicly available on GEO and all other data are available in the main text or the supplementary materials.